Available online at www.sciencedirect.com
SCIENCE DIRECT®
Journal of Molecular Catalysis A: Chemical 236 (2005) 194–205
JOURNAL OF MOLECULAR CATALYSIS A: CHEMICAL
www.elsevier.com/locate/molcata

DFT—Quantum chemical study of the HZSM-5-cyclohexene interaction pathways

Angeles Cuán [a,b,*], José Manuel Martínez-Magadán [a], Isidoro García-Cruz [a], Marcelo Galván [b]

[a] *Programa de Ingeniería Molecular, Instituto Mexicano del Petróleo, Eje Lázaro Cárdenas 152, México 07730, D.F., Mexico*
[b] *Departamento de Química, División de Ciencias Básicas e Ingeniería, Universidad Autónoma Metropolitana-Iztapalapa, A.P. 55-534, México 09340, D.F., Mexico*

Received 10 August 2004; received in revised form 4 April 2005; accepted 5 April 2005

Abstract

A theoretical analysis of the interaction between cyclohexene and a HZSM-5 zeolite model system is presented. Two different models were used to represent this catalyst: a ring structure model consisting of 10 $-TO_4-$ tetrahedral sites (where T = Si, Al) and a smaller model containing 3 $-TO_4-$ tetrahedral sites. Two different reaction pathways were studied: the hydrogen exchange between the HZSM-5 cluster model and the cyclohexene molecule, and the proton addition to double bond of the cyclohexene. The alkoxy species can be stabilized/destabilized depending of the arrangement restriction between the olefin and the local geometry of the active site. When cyclohexene molecule interacts with the 3T model the reaction involves an alkoxy species formation. Due to the allowed relaxation in the ring framework around the active site, the local arrangement restriction of the alkoxy species and therefore the covalent alkoxy bond is too weak giving rise to a more ionic intermediate species (carbenium ion-like), which is characterized as a minimum in the PES. By using the non-interacting system, as a reference, and based on the calculated changes in the total energy of the different complexes, one is able to determine that both carbenium ion-like and alkoxy species are destabilized with respect to physisorbed complexes.

Keywords: Density functional calculations; Catalysis; Zeolites; Cyclic olefins; Carbenium ion; Alkoxy species

1. Introduction

Many studies have been performed to identify different reaction pathways involved in the chemisorption of olefins on zeolites, but there is still some controversy on the details of the interaction. Experimental information supports the general idea that a hydrocarbon reaction on zeolites involves the formation of a carbenium ion-like transition state which is stabilized trough the formation of an alkoxy covalent species as intermediate [1–3]. For example, NMR spectroscopy experiments on dehydration of *tert*-butyl alcohol [4] suggest carbocation formation, since the characterization of an alkoxy species as stable intermediate indicates that this pathway is the most likely one; indeed, the potential energy diagram for this chemical reaction, suggests that the carbocation ion-like formation must be energetically close to the alkoxide complex species [4]. However, not all olefins have such behavior. In fact, in the case of 1-octene adsorbed on HZSM-5 zeolite, there is no evidence of the NMR frequency characteristic of alkoxy group [5]. On the other hand, IR studies for *cis*- and *trans*-2-butenes on deuterated faujasite show that the double-bond migration occurs through H/D isotope exchange reaction of the OH(OD) groups of the Broensted acid site (BAS). These studies suggest that the protonated intermediate is essential for the reaction (alkoxy or carbenium ion-like) on a weak BAS, but no for the ZSM-5 and morden-

* Corresponding author. Tel.: +52 55 9175 8196; fax: +52 55 91 75 62 39.
E-mail addresses: angelescuan24@yahoo.com.mx, acuan@www.imp.mx (A. Cuán).

1381-1169/$ – see front matter © 2005 Elsevier B.V. All rights reserved.
doi:10.1016/j.molcata.2005.04.021

ite (MOR), where the reaction path could not be interpreted by the conventional acid-catalyzed mechanism [6]. Most of the experimental studies showed that the carbenium ion inside the zeolite channels is not a stable species; but lately, some cyclic cations have been experimentally observed to be important long-lived intermediates in some reactions of hydrocarbons on zeolites [7,8]. This experimentally observed cyclic ions stabilization is related to the steric impediment to access the zeolite oxygens framework that induces the positive charge delocalization in the interacting molecule. In other cases, such as the adsorption and reactions of *iso*-butylene on HY and HZSM-5 [9] or H-mordenite [10], neither the *tert*-butyl carbenium ion nor the *tert*-butoxide covalent species have been experimentally observed and, consequently, the nature of the reaction intermediates in this case is not clear yet.

Several theoretical studies have been reported for olefin chemisorption on acidic zeolites [3,11–13]. These works provide valuable information on how an olefin adsorbed on a zeolite acid Broensted site is readily protonated; it is interesting to notice that, for stabilize the positive charge of the carbenium ion-like transition state, an alkoxy bond between the carbon atom of the olefin and one oxygen atom of the zeolite catalytic site is formed [11,13–19]. Recently, Boronat et al. [20] mentioned that in molecules like isobutylene, and depending on the different positions of the aluminum atoms within the MOR framework and on the local geometry of the acid site, the reaction intermediates of olefin protonation involve covalent alkoxides as well as carbenium ions intermediates. The carbenium ion intermediate, can be converted or not, depending on the T position at which the Al atom is located in the zeolite, into the covalent *tert*-butoxide species through a different transition state; indeed, their results [20] indicate that the carbenium ions formed are characterized as minima in the potential energy surface (PES) and that its formation requires considerable energy cost.

It is known that in the interactions between the zeolite framework and the carbocationic transition state complexes first-neighbor electrostatic effects [18] are crucial. Also, the complete zeolite crystal electrostatic contributions for the stabilization energies of carbocationic transition states are not negligible. Previous cluster calculations [13,14], in which a small cluster fragment terminated with hydrogen atoms has been used, suggest that the alkoxy species could be stable reactive intermediates. Nevertheless, it is reported elsewhere [16–18,20] that the adsorbed alkoxy species seems to become as unstable as the protonated hydrocarbons if an improved catalyst model is used. This indicates that the steric constraints provided by the zeolite framework play an important role and that the stabilization of the adsorbed complexes is very sensitive to the local site geometry. With regard to the cluster approach, Boronat et al. [21] also reported that if the cluster model is improved, the activation energies calculated are close to those obtained with the periodic approach. So, the results obtained by means of cluster approach could offer reliable thermodynamic and kinetic data, comparable to those of periodic calculations [18,21–23], if the cluster used is large enough to include all short-range interaction between the molecule and the catalyst. Furthermore, when density functional theory (DFT) is employed, a description comparable to HF/MP2 level of theory is obtained, as has been reported [21,22].

Because our main interest is to describe the local phenomena, this study has been performed using the cluster model approach scheme. The interaction of cyclohexene molecule with the H-ZSM-5 zeolite has been modeled by 3 $-TO_4-$ and 10 $-TO_4-$ cluster models containing either 3 or 10 tetrahedral sites. The 10T-cluster model takes into account some interactions that the 3T-model ignores, and the effect of these differences in the energy profiles is analyzed. In addition, two reaction profiles (one for the hydrogen exchange and the other for the proton addition to double bond of the cyclohexene) are presented. The stability of intermediate species formed on the reaction pathways is discussed in detail for the different models employed. In particular, cyclohexene has been used as model molecule for hydrogen transfer and isomerization reactions [24,25] and it is representative of cyclic olefin compounds in the feed of the fluid catalytic cracking (FCC) process. Theoretical calculations of the reaction pathways involving cyclic olefins and a zeolite model have not been deeply studied yet. Due to the observed differences in the olefins reaction mechanisms [4–10,26–32], it is important to gain insight on the mechanism for proton addition of cyclic olefins over zeolites.

2. Methodology

The electronic structure study includes all-electrons within the Kohn–Sham implementation of density functional theory (DFT). The level of theory used in this work corresponds to the non-local functional developed by Becke, Lee–Yang–Parr (BLYP) [33] whereas the Kohn–Sham orbitals are represented by a double-ζ numerical polarized (DNP) basis set; this is a double-ζ numerical basis set augmented by polarization functions [34]. These bases sets are given as numerical values on a sufficiently large grid centered on each atom. Calculations have been carried out using the DMol^3 computer program coupled to the Accelrys package [35]. The BLYP functional was selected because a non-local functional is required to get reliable energetic profile. In addition, the numerical functions reduce the basis set superposition error, which tends to jeopardize interaction energy calculations. It is known that the BLYP/DNP level of theory gives a suitable description of transition states, in agreement with experimental results, for proton exchange reaction in zeolites [36].

The 3 $-TO_4-$ and the 10 $-TO_4-$ tetrahedral sites structure models were taken from previous studies [37]. These models contain an active site region represented by a Broensted acid site, see Fig. 1. The oxygen atoms bonded to every T atom of the $-TO_4-$ unit are in tetrahedral positions. The dangling

bonds, which would connect the cluster with the rest of the solid structure from the MFI zeolite [38], were saturated with hydrogen atoms.

The non-interacting optimized cyclohexene molecule and the free catalyst model, hereafter referred to as free-fragments (FF), were used as reference for the energy profiles. In the acid Broensted site the whole $-SiO_3AlOHSi-$ environment was fully optimized in both catalyst models. In a similar way, for the different complexes formed in the reaction pathways, the –SiOAlOHSi– region and the cyclohexene molecule were fully relaxed. In the case of the TS, the full-relaxed structure has some spurious normal modes with small negative frequencies. These spurious normal modes disappear when the vibrational analysis is recalculated in a more restricted environment, –OAlOH–. It is important to notice that, in the restricted space, the stationary point corresponds to a TS situation and that the changes in geometry between the –SiOAlOHSi– and –OAlOH– saddle points environments are negligible.

3. Results and discussion

3.1. Active site representation

Boronat et al. [21] have shown that, when the cluster approach is used, the complete optimization of all the geometric parameters of the system should not be carried out since it will yield unrealistic energies and, also that if the cluster model is improved, the activation energies calculated can be very close to those obtained with those arising from a periodic approach. Based on this assumption, and in order to improve the model used, in the present work instead of using a small cluster fragment terminated with hydrogen atoms, the neighbor oxygen atoms binding to the (–SiOAlOHSi–) local site of the zeolite crystal are included. These oxygen atoms are saturated with hydrogen atoms in both models as depicted in Fig. 1. The proton affinities (PAs) calculated for the two clusters models are 337.49 kcal/mol for the small 3T HZSM-5 cluster and 334.47 kcal/mol for the 10T HZSM-5 ring structure. These values overestimate the PAs reported in experimental works by around 5%; experimental determinations are on the range of 280–320 kcal/mol [39].

Starting from the ring structure model, the $-SiO_3AlOHSi-$ region was optimized. The final structure is displayed in Fig. 1a. Due to the fact that the HZSM-5 has not a symmetric structure even for one cage-window, the acidic proton in HZSM-5 has an energetically preferential position for the oxygen which is bonded to the catalytic site. Therefore, the acidic proton prefers to be attached to the O7 oxygen atom rather than to O8 by a small difference of only 1.02 kcal/mol for the small 3T model and by 2.64 kcal/mol in the case of using the 10T-ring structure, Fig. 1. The difference between the 3T-cluster and the 10T-cluster energy values already indicates that the 3T-model ignores some interactions which are present in the larger model. Therefore, the different complexes formed along the reaction pathways were calculated by considering that the acidic hydrogen is attached to the O7 position.

On the other hand, it is well known that the curvature of the zeolite surfaces induces steric constraints that could stabilize/destabilize the adsorption of the reacting molecules [18,20,40,41]. When a small cluster model terminated with hydrogen atoms is used and only the hydrogen capping atoms are fixed; the model cannot be a representation of a particular zeolite. Therefore, the model cannot explain changes in the catalytic behavior due to structural differences. In order to improve the geometry of the 3T-cluster model, this was taken out from the optimized 10T-ring and then the $-SiO_3AlOHSi-$ region was re-optimized. With this proce-

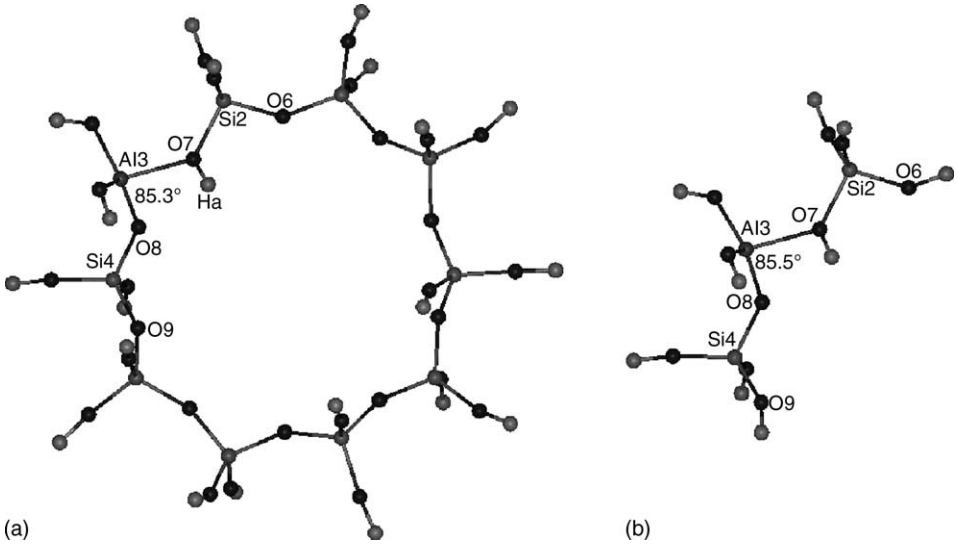

Fig. 1. (a) 10T-HZSM-5 cluster model (10T-model); and (b) 3T-HZSM-5 cluster model (3T-model) used to simulate the active site of the zeolite. These contain 10 and 3 tetrahedral units, respectively.

Table 1
Selected structural parameters, in Å and degrees, for the stationary points of the reaction profiles for hydrogen exchange (Ex) and protonation of cyclohexene (AlkoF)

Parameter	FF		Adsorbed cyclohexene				Transition state		Products			
	3T	10T	3T_Ad_Ex	10T_Ad_Ex	3T_Ad_AlkoF	10T_Ad_AlkoF	3T_TS_Ex	10T_TS_AlkoF	3T_Prod_Ex	10T_Prod_Ex	3T_Prod_AlkoF	10T_Prod_AlkoF
O7─Ha	0.98	0.98	0.98	0.99	0.99	0.99	1.47	2.07	–	–	2.71	3.11
O8─H1	–	–	–	–	–	–	–	–	0.98	0.98	–	–
C1─C2	1.34		1.34	1.35	1.35	1.34	1.36	1.42	1.34	1.34	1.55	1.45
Ha─C1			4.07	3.59	2.79	4.31	1.24	1.15	1.09	1.09	1.09	1.10
Ha─C2			4.51	3.46	2.77	3.89	1.36	1.86	2.11	2.11		2.08
C1─H1	1.09		1.09	1.09	1.09	1.09	1.21	1.10	3.78	3.52	2.18	1.12
O7─C2			5.45	4.98	3.70	4.87	3.54	2.84	5.32	4.98	1.63	2.92
O7─H1			4.49	4.21	3.70	5.14	1.56	3.49	2.17	3.51	3.39	3.87
C2─H2	1.09		1.09	1.09	1.09	1.09	1.09	1.09	1.09	1.09	1.08	1.09
Al3─O7	1.94	1.93	1.97	1.95	1.97	1.95	1.94	1.83	1.76	1.75	2.04	1.79
Al3─O8	1.75	1.75	1.75	1.74	1.74	1.74	1.81	1.79	1.95	1.93	1.73	1.79
Si2─O7	1.69	1.69	1.69	1.69	1.69	1.69	1.63	1.62	1.62	1.62	1.70	1.60
Si4─O8	1.61	1.61	1.61	1.61	1.61	1.61	1.62	1.59	1.68	1.68	1.59	1.58
Al3─C1	∞	∞	5.94	5.62	4.79	6.04	3.70	4.01	5.75	5.62	3.75	4.34
O6─O9	6.59	6.59	6.59	6.59	6.59	6.59	6.59	6.59	6.59	6.59	6.66	6.59
<HaC1H1			52.45	67.80	74.18	78.74	64.71	96.52	49.41	48.80	105.49	99.92
<O7C2H2			–	–	–	–	–	–	–	–	95.61	25.15
<O8Al3O7	85.50	85.30	84.93	84.70	85.11	84.54	88.14	89.83	85.69	85.80	87.36	89.72
<C1C2C3	123.53		123.67	123.79	123.67	123.59	124.44	124.38	123.40	123.55	117.26	124.40
<C1C2H2	119.22		118.75	119.13	118.75	119.10	118.39	115.37	119.42	119.32	107.68	115.40
<C3C2H2	117.26		117.54	117.07	117.54	117.31	117.15	120.23	117.17	117.10	106.71	120.20
<C6C1C2C3	1.4		1.50	0.90	0.09	2.22	1.14	6.26	2.72	0.60	17.10	−14.29
<H1C1C2H2	1.4		0.16	1.50	1.52	1.97	−33.06	−33.44	–	–	–	–

The labels for the structures are explained in Figs. 5 and 7.

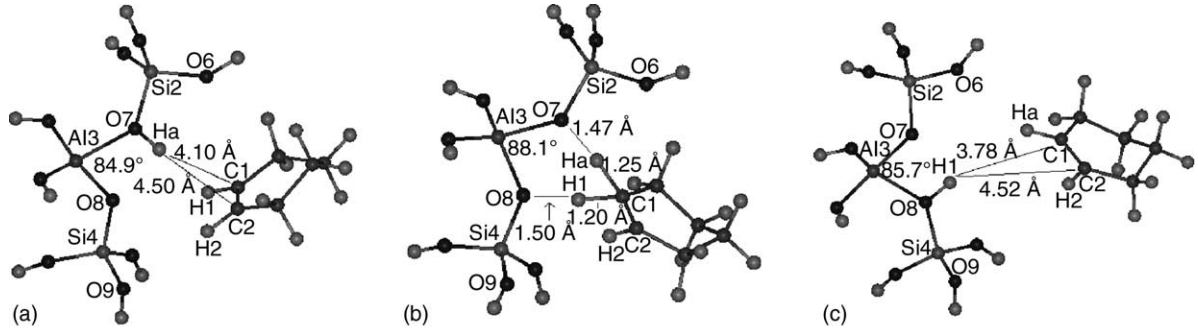

Fig. 2. Stationary points along the reaction coordinate for hydrogen exchange using the small cluster model: (a) adsorbed cyclohexene complex (3T_Ad_Ex); (b) transition state geometry (3T_TS_Ex); and (c) product of the exchange reaction (3T_Prod_Ex).

dure, the 3T-cluster, Fig. 1b, has similar structural parameters than the 10T-ring and, hence, is reminiscent of the HZSM-5 crystal. The most important structural parameters values for the 3T and 10T HZSM-5 models are shown in the first column of Table 1. In the same table, only one aluminium–oxygen distance (Al3–O7) has slightly changed (0.01 Å) in the 3T in comparison with the 10T-ring. The curvature of the cage-window remains invariable in both optimized models.

3.2. Hydrogen exchange

Fig. 2 shows the structures involved in the reaction of hydrogen exchange of cyclohexene catalyzed by the 3T HZSM-5 cluster model. In this reaction cyclohexene interacts with the zeolite model via its double bond side. In Fig. 2b, the calculated transition state, 3T_TS_Ex, for the hydrogen exchange reaction is displayed. The unique imaginary frequency, which has a value of $520.6i\,cm^{-1}$, is identified as a translocation proton event between the zeolite catalyst and cyclohexene.

The 3T_TS_Ex was relaxed in the direction of the reaction coordinate to verify that it connected the adsorbed complex (3T_Ad_Ex) and the product complex (3T_Prod_Ex). The stable complexes related to this reaction pathway are shown in Fig. 2a for reactant, and Fig. 2c for product. In this case, the calculated activation barrier (Ea_1) between the adsorbed complex (3T_Ad_Ex) and the TS complex (3T_TS_Ex) is 76.83 kcal/mol. A slightly stable physisorbed state of the cyclohexene molecule was found. However, given the difficulties of the exchange correlation functionals used in this work to deal with weak interactions, the presence of such a physisorbed state has to be regarded with caution. The calculated adsorption energy, for the adsorbed (3T_Ad_Ex) and product (3T_Prod_Ex) complexes with respect to the FF reference energy, was −0.27 and −0.73 kcal/mol, respectively (see Table 2). The geometric structures for 3T_Ad_Ex and 3T_Prod_Ex correspond to a non-equidistant proton position with respect to the C–C double bond, as Table 1 shows. No important geometrical changes with respect to the FF reference were found between 3T_Ad_Ex and 3T_Prod_Ex complexes; the relevant values for these geometrical changes are shown in Table 1. On the other hand, the C–C double bond distance, and also some internal angles of the cyclohexene molecule for the transition state complex (3T_TS_Ex), have suffered important modifications, which provoked that the C1–C2 double bond distance changed from 1.34 to 1.36 Å, as well as the almost coplanar configuration of the dihedral angle was lost. The H1C1C2H2 angle changed from 1.4° to −33.06°. The new HaC1H1 angle formed in this 3T_TS_Ex complex is 64.7° showing a shift towards a sp^3-like hybridization. In contrast to this, the C2 carbon has geometry close to a planar trigonal like a free carbenium ion. In summary, the cyclohexene environment for the transition state resembles a cyclohexene carbenium ion ($C_6H_{11}^+$). This is qualitatively supported by the Mulliken charge on the $C_6H_{11}^+$ group in the 3T_TS_Ex which is of +0.62 electrons. Table 3 displays the Mulliken charges for some atomic centers for the different complexes involved in this work.

In order to improve the model, the $C_6H_{11}^+$ moiety from the 3T_TS_Ex was embedded in the 10T-ring structure. The merged structure also corresponds to a TS complex, namely 10T_TS_Ex. Fig. 3b displays a schematic representation of the normal mode corresponding to the imaginary frequency

Table 2
Relevant energy differences, in kcal/mol, for the different complexes involved in the hydrogen exchange and proton addition to cyclohexene, employed BLYP/DNP level of theory

Reaction type	Adsorbed cyclohexene (Ad)		Transition state (TS)		Products (Prod)	
	3T_Ad	10T_Ad	3T_TS	10T_TS	3T_Prod	10T_Prod
Hydrogen exchange	−0.27	0.03	76.56	24.55	−0.73	3.34
Cyclohexene protonation	−0.95	0.95	35.03	43.64	20.18	25.75

All the values are calculated taking the non-interacting system as a point of reference.

Table 3
Mulliken charges of some atomic centers for the structures studied in this work

Parameter	FF		Adsorbed cyclohexene				Transition states				Products			
	3T	10T	3T_Ad_Ex	10T_Ad_Ex	3T_Ad_AlkoF	10T_Ad_AlkoF	3T_TS_Ex	10T_TS_Ex	3T_TS_AlkoF	10T_TS_AlkoF	3T_Prod_Ex	10T_Prod_Ex	3T_Prod_AlkoF	10T_Prod_AlkoF
q(O7)	−0.703	−0.711	−0.717	−0.708	−0.747	−0.728	−0.923	−0.922	−0.909	−0.920	−0.895	−0.902	−0.837	−0.906
q(Ha)	0.339	0.344	0.353	0.369	0.386	0.362	0.457	0.346	0.249	0.237	0.115[a]	0.103[a]	0.130	0.177
q(Al3)	1.162	1.154	1.163	1.153	1.161	1.151	1.184	1.186	1.173	1.164	1.157	1.153	1.192	1.151
q(O8)	−0.888	−0.895	−0.892	−0.902	−0.894	−0.901	−0.910	−0.916	−0.911	−0.918	−0.706	−0.708	−0.880	−0.897
q(C1)	−0.064	–	−0.091	−0.107	−0.120	−0.088	−0.570	−0.342	−0.229	−0.230	−0.101	−0.090	−0.176	−0.220
q(H1)	0.055	–	0.105	0.103	0.123	0.063	0.463	0.344	0.199	0.189	0.353	0.362	0.113	0.203
q(C2)	−0.064	–	−0.075	−0.099	−0.119	−0.081	−0.055	0.062	0.128	0.133	−0.069	−0.081	0.146	0.298
q(H2)	0.055	–	0.061	0.090	0.10	0.095	0.238	0.098	0.229	0.223	0.052	0.095	0.171	0.097
q(C3)	−0.162	–	−0.162	−0.174	−0.152	−0.183	−0.445	−0.209	−0.185	−0.211	−0.161	−0.183	−0.127	−0.218
q(H3)	0.084	–	0.080	0.119	0.080	0.105	0.231	0.158	0.164	0.147	0.081	0.105	0.096	0.174
q(H3ĭ)	0.086	–	0.083	0.084	0.085	0.096	0.231	0.107	0.137	0.165	0.079	0.096	0.087	0.179
q(C4)	−0.151	–	−0.148	−0.164	−0.149	−0.168	−0.41	−0.159	−0.152	−0.255	−0.149	−0.168	−0.124	−0.187
q(H4)	0.076	–	0.073	0.070	0.073	0.090	0.215	0.076	0.095	0.159	0.072	0.090	0.076	0.142
q(H4ĭ)	0.076	–	0.068	0.099	0.067	0.092	0.208	0.105	0.096	0.197	0.074	0.092	0.045	0.119
q(C5)	−0.151	–	−0.150	−0.146	−0.154	−0.145	−0.412	−0.152	−0.174	−0.15	−0.150	−0.141	−0.151	−0.157
q(H5)	0.076	–	0.072	0.056	0.069	0.058	0.214	0.068	0.094	0.076	0.074	0.076	0.071	0.087
q(H5ĭ)	0.076	–	0.075	0.063	0.076	0.062	0.208	0.068	0.081	0.070	0.070	0.063	0.067	0.074
q(C6)	−0.162	–	−0.162	−0.153	−0.151	−0.157	−0.433	−0.167	−0.137	−0.157	−0.163	−0.150	−0.118	−0.150
q(H6)	0.084	–	0.082	0.068	0.083	0.068	0.246	0.095	0.098	0.077	0.089	0.070	0.077	0.089
q(H6ĭ)	0.086	–	−0.083	0.083	0.084	0.080	0.238	0.129	0.109	0.141	0.082	0.082	0.068	0.109
q(Org)	0.000	–	−0.006	−0.008	−0.005	−0.013	0.624	0.627	0.802	0.811	0.302	0.318	0.451	0.816

[a] Now the acidic proton is binding to O8.

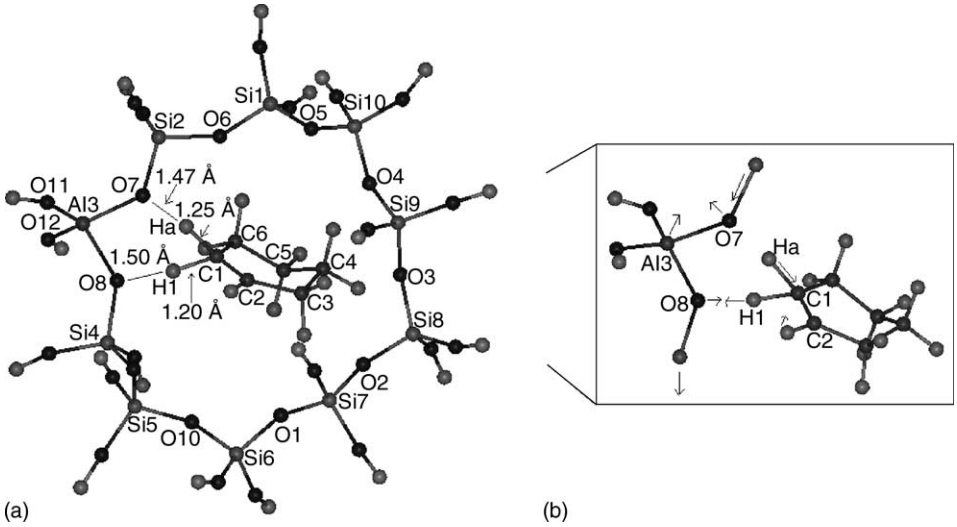

Fig. 3. Transition state geometry, in the ring structure model, involved in the hydrogen exchange reaction profile: (a) corresponds to the TS geometrical structure of 10T_TS_Ex complex and (b) schematically indicates the displacements associated to the imaginary frequency.

of vibration of the transition state, which has a value of 471.9*i* cm^{-1}. It can be observed that protonation of cyclohexene and proton back-donation to the zeolite cluster occurs in a single step. In this case, the embedding TS provokes a decrease of the activation energy of 32% with respect to the result obtained with the 3T-model, which is in the range reported elsewhere [21,41,42].

The 10T_TS_Ex complex was relaxed along the direction of the reaction coordinate to verify if there is a link of the adsorbed complex (10T_Ad_Ex) and the product complex (10T_Prod_Ex). No important differences were found with respect to the formed 3T-cyclohexene complexes. The comparison of the distances and angles for all the complexes involved in the hydrogen exchange reaction, using the two different models, are reported in Table 1. The differences between the isolated cyclohexene, the adsorbed and product complexes (10T_Ad_Ex, 10T_Prod_Ex) are almost negligible. A comparison between Fig. 2a and c with Fig. 4a and b, leads to a difference in the final position of the cyclohexene in the 10T-model compared to the one obtained with the 3T-model. Cyclohexene is slightly closer to the zeolite model in 10T-structure (considering as reference the carbon atom C1, and the aluminum atom Al3) with respect to the 3T-structure (see Table 1).

The calculated activation barrier (Ea_2) between the adsorbed complex (10T_Ad_Ex) and the TS complex (10T_TS_Ex) is of 24.52 kcal/mol. The calculated adsorption energies for the two structures, 10T_Ad_Ex and 10T_Prod_Ex, with respect to the FF, are 0.03 and 3.34 kcal/mol, but the poor performance of DFT for hydrocarbon adsorption energies in zeolites has been noted previously [22]. Nevertheless, the Mulliken charge on the $C_6H_{11}^+$ in the TS

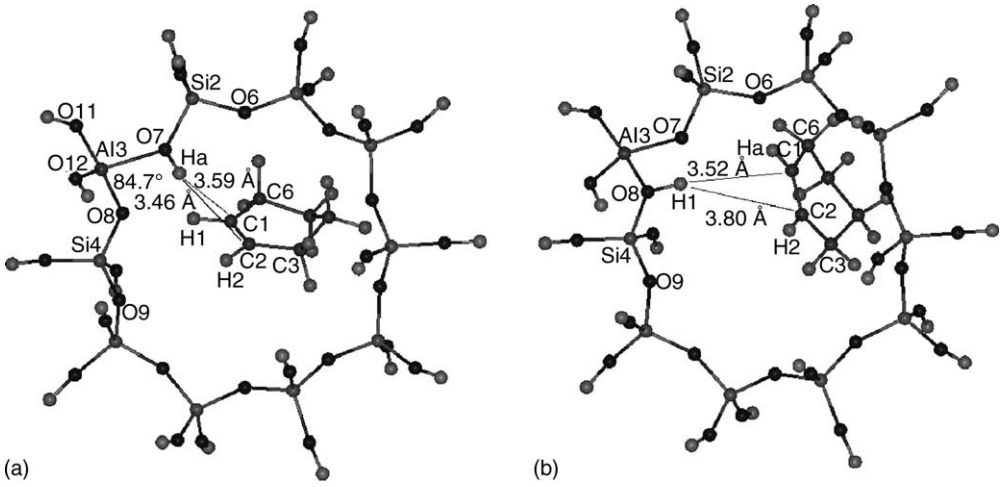

Fig. 4. Stationary points along the reaction coordinate for hydrogen exchange employed the ring structure model: (a) adsorbed cyclohexene complex (10T_Ad_Ex) and (b) exchange product of the reaction (10T_Prod_Ex).

complex (10T_TS_Ex) is +0.63 electrons, similar to the 3T-model.

3.3. Proton addition to double bond

The carbocation formed through olefin protonation has been described in literature [4]. This species is stabilized by the interactions with the catalyst surface, mainly because, upon protonation, an alkoxy bond between a carbon atom of the olefin and an oxygen atom of the zeolite catalytic site is formed. This alkoxy species has been identified as a ground state of a carbenium-ion like in zeolite systems [4,17]. Following this line, the second transition state found in this work corresponds to a proton addition reaction to the double bond in the hydrocarbon molecule and it is related to an alkoxy species formation.

The cyclohexene protonation reaction occurs through a concerted mechanism involving the transition state presented in Fig. 5b, namely, 3T_TS_AlkoF complex. The value for the unique imaginary frequency is $324.3i\,cm^{-1}$, and it is identified with both, the motion of the Ha that is being transferred from the zeolite to the olefin, leading to the formation of a C–H bond (C1–Ha) and the motion of the carbon atom C2 towards to the oxygen atom O7, to form the covalent akoxide bond, as shown in Fig. 5c. In addition, a positive charge transfer is induced to the protonated cyclohexene, $C_6H_{11}^+$, which has a value of +0.80 electrons, see Table 3. The lost of the acidic proton Ha in the catalytic site is compensated by a negative charge on the zeolite framework.

The relaxation of the TS complex (3T_TS_AlkoF), in the direction of the reaction coordinate, connects with the adsorbed complex (3T_Ad_AlkoF) and with the product complex (3T_Prod_AlkoF), Fig. 5a and d, respectively. Such relaxation gives rise to the formation of an alkoxy bond between the zeolite and the hydrocarbon molecule, see Fig. 5d. The difference in energy of stabilization of the alkoxy species with respect to the TS complex (3T_TS_AlkoF) is 14.85 kcal/mol. Nevertheless, the alkoxy product (3T_Prod_AlkoF) is less stable than FF by 20.18 kcal/mol. Such destabilization of the alkoxy product is related to the restriction of the geometry of the cluster to simulate the HZSM-5 particular site [21,22]. The calculated activation barrier (Ea_3), between the adsorbed complex (3T_Ad_AlkoF) and the TS complex (3T_TS_AlkoF) is 35.98 kcal/mol. As was previously pointed out, this value has to be taken with caution due to the failure of the exchange and correlation functional used in this work to describe weak interactions, the calculated adsorption energy for the 3T_Ad_AlkoF complex with respect to the FF is −0.95 kcal/mol, see Table 2. As expected for the small cluster 3T, the TS (3T_TS_AlkoF) involved in alkoxy species formation presents lower activation energy than the TS (3T_TS_Ex) for the hydrogen exchange reaction profile by 40.85 kcal/mol (see Table 2).

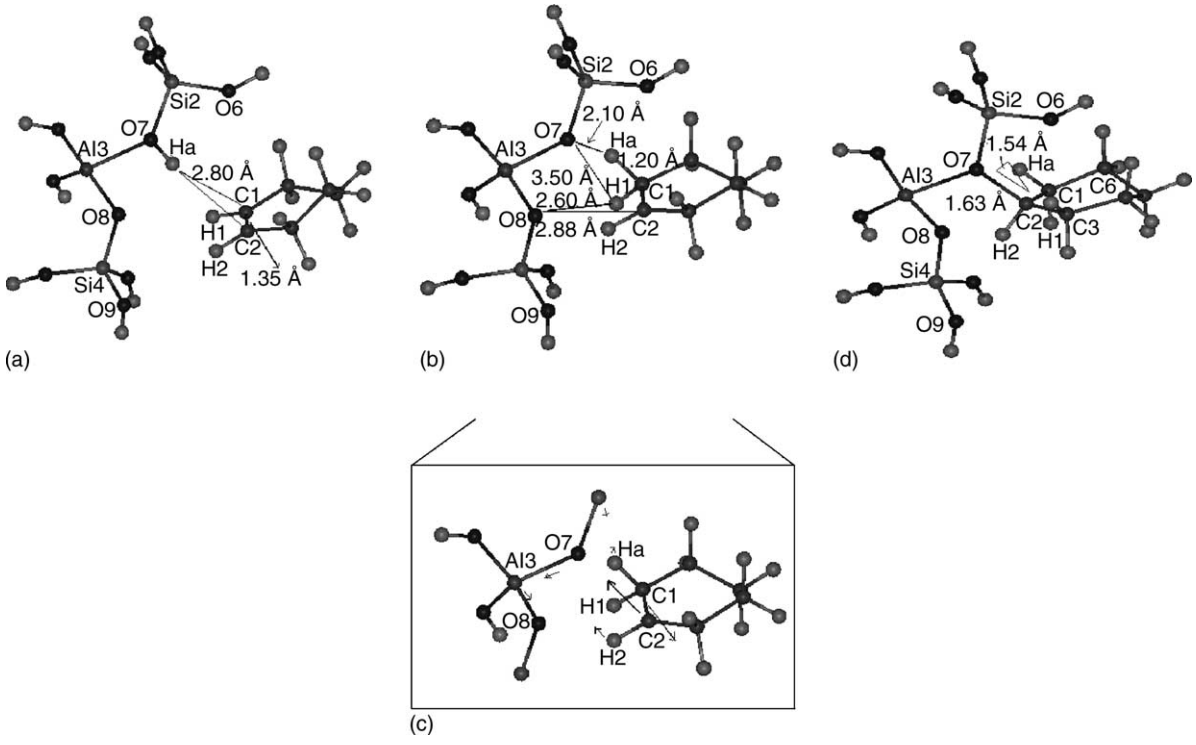

Fig. 5. Stationary points along the reaction coordinate for the alkoxy species formation using the small cluster model: (a) adsorbed cyclohexene complex (3T_Ad_AlkoF); (b) transition state geometry (3T_TS_AlkoF); (c) schematically indicates the displacements associated to the imaginary frequency of the 3T_TS_AlkoF complex and (d) alkoxy species formation as an active intermediate of the reaction (3T_Prod_AlkoF).

None notable geometrical differences have been found between the cyclohexene in the adsorbed complex (3T_Ad_AlkoF) and the cyclohexene as FF, as it is shown in Table 1. But, as expected, the geometry of the transition state complex, 3T_TS_AlkoF, and the alkoxy species, 3T_Prod_AlkoF, have suffered important changes. The values corresponding to the geometrical differences among the FF, 3T_Ad_AlkoF, 3T_Prod_AlkoF and 3T_TS_AlkoF configurations are shown in Table 1. The double bond distance C1–C2 changes from 1.34 Å in the FF to 1.42 Å in the TS complex (3T_TS_AlkoF) and to 1.55 Å in the alkoxy intermediate (3T_Prod_AlkoF). In addition, the almost coplanar configuration of the dihedral angle has been lost: the C6C1C2C3 dihedral angle changes from 1.4° to 6.26° and 17.1°. The HaC1H1 angle formed for the 3T_TS_AlkoF and the 3T_Prod_AlkoF is 96.5° and 105.5°, respectively, showing a larger shift towards a sp^3-like hybridization with respect to the TS complexes (3T_TS_Ex and 10T_TS_Ex) for the hydrogen exchange profile. The bond distance between the oxygen and carbon atom, O7–C1, formed in the alkoxy species complex (3T_Prod_AlkoF) is 1.63 Å. This distance is in the range of the values reported for *sec*-2-butoxide [18], ethoxide [20,21], *n*-butoxide [18] and *tert*-butoxide [14,21] complexes. Similar change in the hybridization of the carbon atom C2 like C1 is observed for the alkoxy intermediate complex. The new O7C2H2 angle formed is 95.61°, as it is depicted in Fig. 5d. The alkoxy species formation (3T_Prod_AlkoF) stabilizes the charge separation from the TS complex (3T_TS_AlkoF) which is +0.45 electrons for the 3T_Prod_AlkoF. Such a value suggests that the nature of the alkoxide–zeolite bond is predominantly covalent, in agreement with literature [14,18,19,21,22].

Next, the $C_6H_{11}^+$ moiety from the TS complex (3T_TS_AlkoF) was embedded in the 10T-ring structure model, namely 10T_TS_AlkoF. The vibrational frequency of the embedded $C_6H_{11}^+$ in the 10T HZSM-5 ring structure also corresponds to a TS complex. Fig. 6b schematically displays the normal mode displacements corresponding to the imaginary frequency of vibration of the transition state, which is 269.7*i* cm^{-1}. The imaginary mode is associated with the motion of the acidic hydrogen Ha towards carbon atom C1 for the C–H bond (C1–Ha) formation. But, in this case the vector of the carbon atom C2 does not point towards the direction of the oxygen atom O7, as in the 3T_TS_AlkoF complex case, as can be seen by comparing Figs. 5c and 6b.

The TS complex (10T_TS_AlkoF) was relaxed along the direction of the reaction coordinate to verify if there is a connection between the adsorbed complex (10T_Ad_AlkoF) and the product complex (10T_Prod_AlkoF), see Fig. 7. The calculated activation barrier (Ea_4), between the 10T_Ad_AlkoF and 10T_TS_AlkoF structures is 42.79 kcal/mol. Again, a poor performance for hydrocarbon physisorption energies is obtained for the 10T_Ad_AlkoF complex and non-relevant differences between the isolated cyclohexene and the 10T_Ad_AlkoF have been found (see Table 1). Nevertheless, the intermediate species as a product (10T_Prod_AlkoF) is 17.89 kcal/mol more stable than the TS complex (10T_TS_AlkoF). Although, that intermediate species is destabilized in relation to the FF by 25.75 kcal/mol. The energy differences for the reaction profiles among the different complexes with respect to the FF are shown in Table 2.

As in the case of the 3T-model (3T_Prod_AlkoF), the intermediate species in the 10T-model (10T_Prod_AlkoF) suffer important changes, see Table 1 and Fig. 7b. The double bond distance C1–C2 changes from 1.34 in the FF to 1.45 Å in the alkoxy species (10T_Prod_AlkoF), and the almost coplanar configuration of the dihedral angle is lost: the C6C1C2C3 dihedral angle changes from 1.4° to −14.29°. The HaC1H1 angle formed for this intermediate (10T_Prod_AlkoF) is 99.9°, showing a smaller shift towards a sp^3-like hybridization with respect to the 3T-model (3T_Prod_AlkoF). The dis-

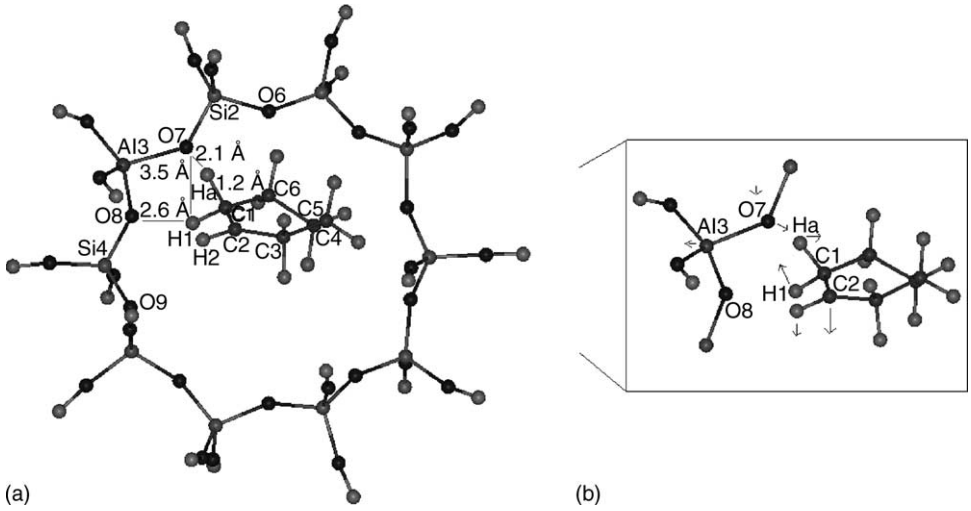

Fig. 6. Transition state geometry, for the protonation of cyclohexene in the ring structure model: (a) corresponds to geometrical structure of 10T_TS_AlkoF complex and (b) schematically indicates the displacements associated to the imaginary frequency.

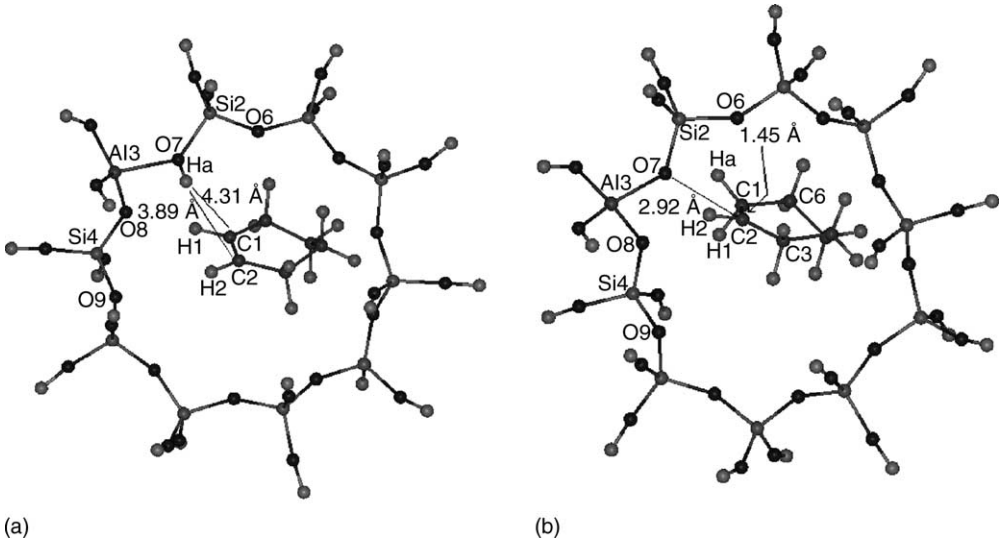

Fig. 7. Stationary points along the reaction, for the protonation of cyclohexene in the ring structure model: (a) adsorbed cyclohexene complex (10T_Ad_AlkoF) and (b) carbenium ion-like formation as an active intermediate (10T_Prod_AlkoF).

tance between the oxygen and carbon atom O7–C2 in the 10T_Prod_AlkoF complex is 2.92 Å.

In contrast to the result of the alkoxy species formation in the 3T-model (3T_Prod_AlkoF), for the formed species in the 10T-model (10T_Prod_AlkoF), the carbon atom C2 almost remains with sp^2 hybridization. The values for the C1C2H2, H2C2C3 and C1C2C3 angles are 115.4°, 120.2° and 124.4°, respectively (Table 1). On its part, the Mulliken charge on $C_6H_{11}^+$ for the 10T_Prod_AlkoF complex is +0.82 electrons, which is rather the same as in the TS complex (10T_TS_AlkoF).

All the structural changes between 3T_Prod_AlkoF and 10T_Prod_AlkoF complexes indicate that the 10T_Prod_AlkoF complex cannot be an alkoxy intermediary product, but it certainly is a more ionic intermediate species (carbenium ion-like), close to a carbenium ion nature. But in this case, the carbenium ion-like is characterized as a minimum in the PES by means of the frequency calculations and its relative position in the PES was confirmed by MP2/DZP(Dunning) single point calculations performed within the NWChem code [43]. The difference found between the two intermediates (alkoxy and carbenium ion-like) is related to the structural changes in the zeolite cluster models (3T and 10T-HZSM-5), as will be discussed in the next section.

3.4. Cluster model size effects

A reduction in the activation energy has been obtained for the hydrogen exchange by embedding of the TS geometry from the small cluster (3T_TS_Ex) into the ring structure (10T_TS_Ex). This reduction is in agreement with the observed results from other systems, in which the activation energy also decreases when the system is embedded in a bigger environment [21,41,42]. Nevertheless, when the 3T_TS_AlkoF is embedded into the ring structure 10T_TS_AlkoF (for the proton addition reaction), the opposite behavior is observed, there is no activation energy reduction for the (3T_TS_ AlkoF in 10T_TS_ AlkoF) embedded system. On the other hand, comparing the stabilization energies for the active intermediaries (10T_Prod_AlkoF, 3T_Prod_AlkoF) with respect to the non-interacting systems, the energy for the 10T_Prod_AlkoF is 5.57 kcal/mol above of 3T_Prod_AlkoF. In contrast, the active intermediary stabilization in 10T_Prod_AlkoF is approximately 3 kcal deeper in energy than the 3T_Prod_AlkoF (see Table 2). This result is closely related to some important geometrical differences for the intermediates species involved in the two different cluster models (3T and 10T-HZSM-5).

In this respect, due to the fact that geometry relaxation is restricted to the (–SiOAlOHSi–) environment, the distance between the oxygen O6 and the oxygen O9 is 6.59 Å in most of the systems (Fig. 1). On its part, for the alkoxy product complex (3T_Prod_AlkoF) such a distance has been modified to 6.66 Å, see Table 1. Then, the geometrical relaxation of the small model allows a better fit of the covalent alkoxy species around the active site, due to the fact that the 3T does not have structural restriction like the 10T ring model, which is restricted by the rest of the zeolite framework. This indicates that the stabilization of the alkoxy species is very sensitive to the local geometry of the active site, as it has been reported elsewhere [18,20–23,41]. It is worthy noticing that the increase in the O9–O6 distance implies that the 3T-model is related to a model with a smaller curvature. Hence, the formation of alkoxy species as intermediary (as the case of 3T-model) is not allowed in the ring model, due to the steric constriction provided by the rest of the framework.

Now, by analyzing the cyclohexene in the 10T_Prod_AlkoF complex, it is found that it is closely related to the structural characteristics like the free car-

benium ion. The distance of 2.92 Å between the atom of carbon and oxygen (C2–O7) in the 10T_Prod_AlkoF is 1.29 Å longer than in 3T_Prod_AlkoF complex, what suggests that covalent binding between them is not achieved. Moreover, the charge separation is not stabilized by the carbenium ion-like in the ring structure (10T_Prod_AlkoF), and it remains like in the TS (10T_TS_AlkoF), around +0.80 electrons in both complexes. Nevertheless, the formation of the carbenium ion-like is characterized as a minimum on the PES and, thus, it can be considered a reactive intermediary, similar result has been reported recently [20]. On the other hand, a considerable energy cost, comparing the energy levels between the 10T_TS_AlkoF and 10T_TS_Ex complexes with respect to the non-interacting systems (FF), is obtained; the corresponding hydrogen exchange TS is lower by 19.1 kcal/mol than the one obtained from the TS for 10T_TS_AlkoF, as can be seen in Table 2. The energy difference can be related for the demanding energy to carbenium ion-like formation. It is expected that many species and mechanisms can be present in the addition of the proton to the olephinic double bond. In this work two of them have been studied. The proton exchange in the double bond of the cyclohexene molecule has not been studied before, and, unless appropriate deuterated species are used, the product and the reactive are the same. Moreover, in this reaction there is no formation of intermediate species to help in the characterization of this mechanism. Unfortunately, there is not experimental data for this specific reaction. Nevertheless, both mechanisms can be present in the reaction pathway, although according to the results in the ring model, the proton addition reaction has a considerable energy cost with respect to the proton exchange reaction.

To close this section we point out that the discussion of this section suggests the formation of the alkoxy compound as an active intermediary sensitive to the local structure of the active site, as it has been reported for other systems [4,18,20–23,41]. Nevertheless, when the alkoxy cannot be stabilized then the formation of a more ionic intermediate species (carbenium ion-like), close to a free carbenium ion nature could be an alternative in the reaction mechanism.

4. Conclusions

In the case of the 3T-HZSM-5-cyclohexene interaction, an alkoxy species (3T_Prod_AlkoF) was found to be more stable by 15.80 kcal/mol than the TS (3T_TS_AlkoF) complex, but less stable by 20.18 kcal/mol than the non-interacting system. The hydrogen exchange reaction between the Ha and the cyclohexene molecule currently presented has been dealt in a non-traditional sense. This has been taken as a comparative result in the study of proton addition to the double bond, which is also important. In this concern, as expected, by embedding the TS geometry from the small cluster (3T_TS_Ex) into the ring structure (10T_TS_Ex), a reduction in the activation energy for the hydrogen exchange has been obtained. When the 3T_TS_AlkoF from the protonation of the cyclohexene is embedded into the ring structure 10T_TS_AlkoF a contrary behavior is observed. This result was related to some geometrical differences for the intermediate products when the cyclohexene interacts with the two different cluster models (3T and 10T-HZSM-5). The geometrical relaxation of the small model (–SiOAlOHSi–) environment, allows the necessary structural changes to accommodate the covalent alkoxy species around the active site. This becomes more difficult when the active site in the catalyst is restricted by the rest of the framework, like in the ring model; hence, the sensibility of the alkoxy product stabilization depends on the local geometry of the active site. Then, the correct representation of the zeolite within the cluster model approach, at least, has to involve one ring structure to take account the curvature effects.

Formation of a more ionic intermediate species, close to a free carbenium ion in nature, is an alternative for the TS stabilization, when the alkoxy species, as a stable reactive intermediate, is not possible. However, one must also notice that, the carbenium ion-like formation and stabilization is the most demanding energy process during the proton addition reaction to the double bond of cyclohexene molecule although it is comparable to the proton exchange reaction for the ring model.

Acknowledgements

A. Cuán acknowledges the Mexican Institute of Petroleum and CONACYT-México for the Ph.D. scholarship. NWChem Version 4.5 as developed and distributed by Pacific Northwest National Laboratory, Richland, WA, USA, and funded by the U.S. Department of Energy, was used to obtain some of the results in this work.

References

[1] J. Scherzer, Catal. Rev.-Sci. Eng. 31 (1989) 215.
[2] W. Wojcechowski, A. Corma, Catalytic Cracking: Catalysts, Chemistry and Kinetics, Dekken, New York, 1986.
[3] V.B. Kazansky, Catal. Today 51 (1999) 419.
[4] R.J. Gorte, D. White, Top. Catal. 4 (1997) 57.
[5] A.G. Stepanov, M.V. Luzgin, V.N. Romannikov, K.U. Zamaraev, Catal. Lett. 24 (1994) 271.
[6] J.N. Kondo, L. Shao, F. Wakabayashi, K. Domen, J. Phys. Chem. B 101 (1997) 9314.
[7] S. Yang, J.N. Kondo, K. Domen, Catal. Today 73 (2002) 113.
[8] S. Yang, J.N. Kondo, K. Domen, Stud. Surf. Sci. Catal. 135 (2001) 12.
[9] N.D. Lazo, B.R. Richardson, P.D. Schettler, J.L. White, E.J. Munson, J.F. Haw, J. Phys. Chem. 95 (1991) 9420.
[10] H. Ishikawa, E. Yoda, J.N. Kondo, F. Wakabayashi, K. Domen, J. Phys. Chem. B 103 (1999) 5681.
[11] A.M. Rigby, G.J. Kramer, R.A. van Santen, J. Catal. 170 (1997) 1.
[12] J.M. Martínez-Magadán, A. Cuán, M. Castro, Int. J. Quant. Chem. 88 (2002) 750.
[13] R.A. van Santen, Catal. Today 30 (1997) 377.

[14] R.J. Correa, C.J.A. Mota, Phys. Chem. Chem. Phys. 4 (2002) 375.
[15] J. Sauer, M. Sierka, F. Haase, ACS Symposium Series 721, American Chemical Society, Washington, 1999, 358 pp.
[16] A.M. Rigby, M.V. Frash, J. Mol. Catal. A 126 (1997) 61.
[17] M.T. Aronson, R.J. Gorte, W.E. Fameth, J. Catal. 105 (1987) 455.
[18] M. Boronat, C.M. Zicovich-Wilson, P. Viruela, A. Corma, Chem. Eur. J. 7 (2001) 1295.
[19] H. Soscun, J. Hernández, O. Castellano, F. Arrieta, F. Ruette, A. Sierralta, F. Machado, M. Rosa-Brusin, J. Mol. Catal. A: Chem. 192 (2003) 63.
[20] M. Boronat, P.M. Viruela, A. Corma, J. Am. Chem. Soc. 126 (2004) 3300.
[21] M. Boronat, M.C. Zicovich-Wilson, P. Viruela, A. Corma, J. Phys. Chem. B 105 (2001) 11169.
[22] S.A. Zygmunt, L.A. Curtiss, P. Zapol, L.E. Iton, J. Phys. Chem. B 104 (2000) 1944.
[23] X. Rozanska, R.A. van Santen, T. Domuth, H. Hutschka, J. Hafner, J. Phys. Chem. B 107 (2003) 1309.
[24] M. Hunger, Catal. Rev.-Sci. Eng. 39 (1997) 345.
[25] U.A. Sedran, Catal. Rev.-Sci. Eng. 36 (1994) 405.
[26] V.J. Rao, N. Prevost, V. Ramamurthy, M. Kojima, L.J. Johnston, Chem. Commun. (1997) 2209.
[27] A. Moissette, S. Marquis, I. Gener, C. Brémard, Phys. Chem. Chem. Phys. 4 (2002) 5690.
[28] M.T. Aronson, R.J. Gorte, W.E. Fameth, D. White, J. Am. Chem. Soc. 111 (1989) 840.
[29] P.B. Venuto, E.L. Wu, J. Catal. 15 (1969) 205.
[30] H. van Bekkum, E.M. Flanigen, J.C. Jansen, Introduction to Zeolite Science and Practice, Studies in Surface Science and Catalysis, vol. 58, Elsevier, Amsterdam, 1991, p. 15.
[31] M.A. den Hollander, M. Wissink, J.A. Moulijn, Appl. Catal. A 223 (2002) 85.
[32] W.E. Fameth, R.J. Gorte, Chem. Rev. 95 (1995) 615.
[33] (a) A.D. Becke, J. Chem. Phys. 88 (1988) 2547;
(b) C. Lee, W. Yang, R.G. Parr, Phys. Rev. B 37 (1988) 786.
[34] B. Delley, D.E. Ellis, J. Chem. Phys. 76 (1982) 1949.
[35] DMol^3 Module of Cerius2, Accelrys Corp., San Diego, CA, 2003.
[36] J.B. Nicholas, Top. Catal. 4 (1997) 157.
[37] J.M. Martínez-Magadán, S. Meléndez-Mercado, R. Santamaría, Chem. Phys. Chem. 11 (2001) 694.
[38] D.H. Olson, G.T. Kokotailo, S.L. Lawton, W.M. Meier, J. Phys. Chem. 85 (1981) 2238.
[39] J. Datka, M. Boczar, P. Rymarowics, J. Catal. 114 (1988) 368.
[40] F. Haase, J. Sauer, Micropor. Mesopor. Mater. 35 (2000) 379.
[41] A.M. Vos, X. Rozanska, R.A. Shchoonheydt, R.A. van Santen, H. Hutschka, J. Hafner, J. Am. Chem. Soc. 123 (2001) 2797.
[42] J.M. Vollmer, T.N. Truong, J. Phys. Chem. B 104 (2000) 6308.
[43] High Performance Computational Chemistry Group, NWChem, A Computational Chemistry Package for Parallel Computers, Version 4.5, Pacific Northwest National Laboratory, Richland, WA, USA, The basis set used was the internal DZP(Dunning).